Published in final edited form as:
Neuron. 2008 May 8; 58(3): 374–386. doi:10.1016/j.neuron.2008.02.029.

Ca^{2+}/calmodulin-mediated fast desensitization by the B1b subunit of the CNG channel affects response termination but not sensitivity to recurring stimulation in olfactory sensory neurons

Yijun Song[1,2], **Katherine D. Cygnar**[1], **Botir Sagdullaev**[3], **Matthew Valley**[3], **Sarah Hirsh**[1], **Aaron Stephan**[1], **Johannes Reisert**[4,*], and **Haiqing Zhao**[1,*]

1*Department of Biology, The Johns Hopkins University, Baltimore, MD 21218*

2*Department of Neurology & Tianjin Neurological Institute, Tianjin Medical University General Hospital, Tianjin, 300052, China*

3*Department of Biological Sciences, Columbia University, New York, NY 10027*

4*Monell Chemical Senses Center, Philadelphia, PA 19104*

Summary

Ca^{2+}/calmodulin-mediated negative feedback is a prototypical regulatory mechanism for Ca^{2+} permeable ion channels. In olfactory sensory neurons (OSNs) such regulation on the cyclic nucleotide-gated (CNG) channel is considered a major mechanism of OSN adaptation. To determine the role of Ca^{2+}/calmodulin desensitization of the olfactory CNG channel, we introduced a mutation in the channel subunit CNGB1b in mice that rendered the channel resistant to fast desensitization by Ca^{2+}/calmodulin. Contrary to expectations, mutant OSNs showed normal receptor current adaptation to repeated stimulation. Rather, they displayed slower response termination and consequently, a reduced ability to transmit olfactory information to the olfactory bulb. They also displayed reduced response decline during sustained odorant exposure. These results suggest that Ca^{2+}/calmodulin-mediated CNG channel fast desensitization is less important in regulating the sensitivity to recurring stimulation than previously thought and instead functions primarily to terminate OSN responses.

Keywords

olfaction; signal transduction; adaptation; CNG channel; calcium channel

Introduction

Olfactory sensory neurons (OSNs) convert odor stimuli into cellular electrical signals. In vertebrates, olfactory signal transduction takes place within OSN cilia extending from the dendritic knob, a distal swelling of the dendrite, into the mucus of the nasal cavity. Odor stimulation, via a G protein-coupled cascade, elevates the cilial concentration of cAMP, which directly binds to and opens the olfactory cyclic nucleotide-gated (CNG) channel. The resulting influx of Na^{+} and Ca^{2+} depolarizes the OSN (for review, see Firestein, 2001) (Firestein,

*.Corresponding authors.

2001). Ca^{2+} further opens a Ca^{2+}-activated Cl^- channel, causing efflux of Cl^- and additional membrane depolarization (Kleene, 1993; Kurahashi and Yau, 1993; Lowe and Gold, 1993; Reisert et al., 2005). The depolarization, or receptor potential, triggers action potentials that propagate along the OSN axon to the olfactory bulb (OB) in the brain.

In addition to generating the initial electrical response, the olfactory CNG channel is also a target for negative feedback regulation. Ca^{2+} that enters the cilium through CNG channels is thought to bind to calmodulin (CaM) associated with the CNG channel (Bradley et al., 2004), reducing the cAMP sensitivity of the CNG channel and leading to channel closure. Desensitization of the CNG channel by Ca^{2+}/CaM was demonstrated in excised membrane patches from dendritic knobs of OSNs (Chen and Yau, 1994). However, the physiological significance of how this negative feedback mechanism regulates the OSN cellular response remains speculative, especially as *in vivo* "loss-of-function" studies have not been performed.

Mammalian OSNs respond rapidly to stimulation and the response terminates quickly once the stimulus ends. Like many other sensory receptor cells, OSNs adapt in response to repeated or sustained stimuli. Experimentally, OSN adaptation is manifested as a reduced electroolfactogram (EOG, the transepithelial potential changes resulting from summed receptor potentials of OSNs (Scott and Scott-Johnson, 2002)) and receptor current response to the second stimulus when exposed to two consecutive odorant pulses, or a progressive reduction of the response during a sustained odorant presentation. These two manifestations of adaptation are thought to rely on different yet overlapping sets of molecular mechanisms (Leinders-Zufall et al., 1999; Zufall and Leinders-Zufall, 2000). The Ca^{2+}/CaM desensitization of the CNG channel has been inferred to be the dominant mechanism of OSN adaptation to repeated stimulation (Boccaccio et al., 2006; Kurahashi and Menini, 1997; Leinders-Zufall et al., 1999; Munger et al., 2001), and also to play a role in adaptation during sustained stimulation (Munger et al., 2001) (for clarity we use the term "desensitization" to refer exclusively to the reduction of sensitivity of the CNG channel to cAMP and the term "adaptation" to describe the cellular phenomenon of decreased OSN responsiveness to repeated or during sustained stimulation).

To determine the role of the Ca^{2+}/CaM-mediated CNG channel desensitization in regulating OSN responses, we sought to interrupt the Ca^{2+}/CaM-CNG channel interaction *in vivo*. Presently, no pharmacological reagents are known that can selectively block Ca^{2+}/CaM binding to the CNG channel without affecting other Ca^{2+}/CaM targets in the signal transduction pathway, such as Ca^{2+}/CaM-dependent phosphodiesterase 1C (PDE1C) (Yan et al., 1995) and Ca^{2+}/CaM-dependent protein kinase II that phosphorylates adenylyl cyclase III (ACIII) (Wei et al., 1998). We therefore introduced a mutation in the channel that abolishes CaM binding. The native olfactory CNG channel is a heterotetramer, consisting of one CNGB1b, one CNGA4, and two CNGA2subunits (Bonigk et al., 1999; Kaupp and Seifert, 2002; Zheng and Zagotta, 2004). cAMP binds to the intracellular C-terminal region of each subunit and promotes channel opening. CaM-binding domains, present in each subunit, reside in the intracellular N-terminal region of the A2 (Liu et al., 1994) and B1b subunits (Grunwald et al., 1998; Trudeau and Zagotta, 2002; Weitz et al., 1998), and in the intracellular C-terminal region of the A4 subunit (Bradley et al., 2004). Among these CaM-binding domains in the tetrameric channel, targeted mutagenesis and heterologous expression showed that only the sites in the B1b and A4 subunits are critical for Ca^{2+}/CaM-mediated desensitization. Deletion of the CaM-binding domain in the B1b subunit alone renders heterologously expressed A2/A4/B1b$^{\Delta CaM}$ channels insensitive to Ca^{2+}/CaM (Bradley et al., 2004). We therefore reasoned that the native channel on the OSN cilia with a similar CaM-binding domain deletion in the B1b subunit should be resistant to desensitization by Ca^{2+}/CaM.

We have used gene targeting to generate a mouse strain, CNGB1$^{\Delta CaM}$, in which the CNGB1b channel subunit lacks the N-terminal CaM-binding domain. We show that native olfactory CNG channels with this mutation have normal cilial localization and sensitivity to cAMP and, as expected, lack fast desensitization by Ca^{2+}/CaM. OSNs with the mutant channel display normal sensitivity and onset kinetics upon initial odorant exposure. Unexpectedly, in a paired-pulse paradigm, CNGB1$^{\Delta CaM}$ OSNs showed EOG and receptor current adaptation similar to wild type OSNs. This result contrasts with the reported role of Ca^{2+}/CaM desensitization of the CNG channel in mediating adaptation to repeated stimulation. Instead, we found that the EOG and the receptor current declined more slowly after stimulation ceased, revealing that Ca^{2+}/CaM desensitization of the CNG channel plays an important role in OSN response termination. Presumably as an effect of prolonged termination, CNGB1$^{\Delta CaM}$ OSNs exhibited a compromised ability to transmit olfactory information to the OB. CNGB1$^{\Delta CaM}$ OSNs also displayed reduced response decline during sustained odorant exposure, suggesting that Ca^{2+}/CaM desensitization of the CNG channel contributes to this form of adaptation. Together, our data suggest that Ca^{2+}/CaM-mediated fast desensitization of the CNG channel plays a less important role in regulating receptor potential/current amplitudes to recurring stimulation than previously thought, and instead functions primarily to terminate the OSN response during and after stimulation.

Results

Generation of CNGB1$^{\Delta CaM}$ mice

The CNGB1b channel subunit is an olfactory specific isoform encoded by the *Cngb1* gene (Sautter et al., 1998). To disrupt the Ca^{2+}/CaM-mediated desensitization of the olfactory CNG channel *in vivo*, we constructed a gene-targeting vector to delete the coding sequence for amino acids LQELVKMFKERTEKVKEKLI, which constitute the N-terminal IQ type CaM-binding domain of the CNGB1b subunit, in the *Cngb1* gene from the mouse genome based on homologous recombination (Figure 1A). In this targeting vector, a loxP-flanked neomycin resistance (LNL) cassette for drug selection of recombination was placed in the intron downstream of the exon coding CaM-binding domain at a site away from the consensus splicing sequence. The LNL cassette was subsequently removed from the CNGB1$^{\Delta CaM}$ genome by crossing with CMV-cre transgenic mice (Schwenk et al., 1995), minimizing the alteration to the *Cngb1* allele to ensure a normal level of expression. The lack of the CaM-binding domain coding sequence in the CNGB1$^{\Delta CaM}$ genome was confirmed by sequencing of the PCR product spanning the deletion site (Figure 1B). The CNGB1$^{\Delta CaM}$ mice had normal growth rate and showed no obvious behavioral abnormalities.

To ensure that any physiological phenotypes are not due to altered expression or mislocalization of the mutant CNG channel, we examined the protein level and cellular localization of each CNG channel subunit in OSNs of CNGB1$^{\Delta CaM}$ mice. The CNGB1$^{\Delta CaM}$ olfactory epithelium (OE) showed no difference from the wild type OE in gross morphology. Immunostaining on cryosections of the OE demonstrated that all three CNG channel subunits as well as other signal transduction components such as ACIII and PDE1C were all properly located at the cilial layer (Figure 1D). Western blot analysis of total epithelial protein further showed that the CNGB1$^{\Delta CaM}$ OE had similar protein levels to the wild type OE for each channel subunit and ACIII (Figure 1C). We concluded that the CNGB1$^{\Delta CaM}$ mice had no apparent defects in expression and localization of olfactory transduction components.

The CNG channel in CNGB1$^{\Delta CaM}$ OSNs has normal sensitivity to cAMP, but lacks fast desensitization by Ca^{2+}/calmodulin

We anticipated that the native channel from CNGB1$^{\Delta CaM}$ OSNs would lack Ca^{2+}/CaM desensitization similar to heterologously expressed A2/A4/B1b$^{\Delta CaM}$ channels (Bradley et al.,

2004). To test this, we conducted patch-clamp experiments on excised membrane patches from dendritic knobs of dissociated OSNs. cAMP-induced current increased similarly in a dose dependent manner in both wild type and CNGB1$^{\Delta CaM}$ membrane patches (Figure 2A). The mean currents induced by saturating concentration of cAMP (100 μM) are comparable between the two genotypes (Wild type, 216±62 pA (mean±SEM), n=8; CNGB1$^{\Delta CaM}$, 215±41 pA, n=20) (Figure 2B inset), indicating a similar CNG channel density. The cAMP dose-response relations of the two genotypes were virtually identical (Figure 2B), suggesting that the CNGB1$^{\Delta CaM}$ channel retains normal sensitivity to cAMP (also for cGMP, data not shown). In the presence of Ca^{2+} (100 μM), calmodulin (1 μM) perfusion abruptly decreased cAMP (6 μM)-induced current in wild type patches, but had no immediate effect on the current in CNGB1$^{\Delta CaM}$ patches (Figure 2C), demonstrating that the mutant CNG channel in CNGB1$^{\Delta CaM}$ mice lacked fast desensitization by Ca^{2+}/CaM. The CNGB1$^{\Delta CaM}$ channel exhibited only a slow desensitization with kinetics around 100-fold slower than the fast desensitization.

The normal level of channel expression and cAMP sensitivity, together with the correct cilial localization of the mutant channel in CNGB1$^{\Delta CaM}$ OSNs, allows us to attribute any physiological defects to the loss of fast desensitization by Ca^{2+}/CaM alone.

CNGB1$^{\Delta CaM}$ OSNs show normal sensitivity to odorant stimulation

Given the normal cilial localization and cAMP sensitivity of the mutant channel, we expected CNGB1$^{\Delta CaM}$ OSNs to have normal sensitivity to odorant stimulation. Alternatively, if a portion of CNG channels in the wild type are desensitized by Ca^{2+}/CaM in the unstimulated state, the sensitivity of CNGB1$^{\Delta CaM}$ OSNs could be increased. To investigate whether elimination of the Ca^{2+}/CaM-binding site on the B1b subunit of the CNG channel alters the odorant sensitivity of OSNs, we measured the OSN response to brief odorant pulses (100 ms) using the electroolfactogram. In our recording setup, odorants were delivered in the vapor phase to the OE surface. We tested two commonly used odorants, amyl acetate and heptaldehyde, and present the data in most cases only for amyl acetate, as the two odorants produced similar results. Figure 3A shows EOG amplitudes to the vapor of a 10^{-4} M amyl acetate solution (~EC_{50} concentration of the dose-response relation, see below) from 11 locations across the turbinate IIb and III. The EOG amplitude varied similarly at different recording locations, but there was no difference between the wild type and the CNGB1$^{\Delta CaM}$ in comparable locations. Figure 3B shows the dose-response relation measured at a fixed location on turbinate IIb (position one as indicated in Figure 3A). The wild type and CNGB1$^{\Delta CaM}$ OE generated similar maximum EOG amplitudes (wild type: 21.0±4.9 mV (mean±SD), n=6 mice; CNGB1$^{\Delta CaM}$: 19.2±7.5 mV; n=6 mice) and had virtually identical dose-response relations with EC_{50} concentration slightly above 10^{-4} M. Further analysis of EOG signals showed no significant difference in the latency and rise time between wild type and CNGB1$^{\Delta CaM}$ OSNs ($p>0.05$) in response to the same concentration of odorant (Table 1). This finding allows us to compare wildtype and mutant OSN responses at the same odorant concentration.

CNGB1$^{\Delta CaM}$ OSNs exhibit normal adaptation to repeated odorant exposure

A brief odorant exposure is sufficient to adapt an OSN, such that an identical exposure occurring shortly thereafter evokes a reduced response. Since Ca^{2+}/CaM-mediated CNG channel desensitization is thought to be the dominant mechanism for OSN adaptation to repeated stimulation (Boccaccio et al., 2006; Kurahashi and Menini, 1997; Munger et al., 2001), an expected consequence of the loss of this negative feedback mechanism would be a failure to show adaptation to the second stimulus. To test this, we examined OSN responses in a paired-pulse stimulation paradigm. Figure 4A shows averaged EOG signals induced by two consecutive 100 ms pulses from the vapor of 10^{-4} M amyl acetate solution separated by intervals as short as 1 second (for analysis of the slowed termination phase see below). The

response to the second pulse is reduced to almost half of the response to the first pulse in wild type OE. In contrast to expectations, CNGB1$^{\Delta CaM}$ OSNs exhibited the same reduced amplitude as the wild type OSNs. Similar results were observed for higher amyl acetate concentrations of 10^{-3} M and 10^{-2} M, as well as for the second odorant heptaldehyde (Figure 4B).

Adaptation can be further quantified by the shift of the dose-response relation after an adapting stimulus. We measured the dose-response relation for amyl acetate at the 1 second time point after a 2-second 10^{-4} M conditioning stimulation. CNGB1$^{\Delta CaM}$ and wild type OSNs exhibited similarly reduced responses to the test pulses and had equally shifted dose-response relations with an approximate EC_{50} concentration increased by one order of magnitude (Supplemental Data Figure S1).

We further confirmed that CNGB1$^{\Delta CaM}$ OSNs had normal adaptation to repeated stimulation at the single cell level using IBMX (3-isobutyl-1-methyl-xanthine), a phosphodiesterase inhibiter commonly used to induce receptor currents in single cell studies (IBMX induces receptor currents in OSNs by inhibiting the basal activity of cilial phosphodiesterase and hence elevating cAMP levels), or the odorant cineole as stimulants. Figures 4C and D show suction current responses to a pair of 1-second stimulus pulses with various interpulse intervals ranging from 10 to 0.25 seconds. Stimulation with either IBMX (Figure 4C) or cineole (Figure 4D) caused adaptation in wild type OSNs. The suction current to the second pulse was progressively reduced as the interpulse intervals were shortened. Consistent with the EOG results, CNGB1$^{\Delta CaM}$ OSNs displayed similar adaptation as the wild type OSNs. The averaged ratios of the second response to the first were not different between the two genotypes for all equivalent stimulus pairs, suggesting that the extent of adaptation and the rate of recovery from adaptation in CNGB1$^{\Delta CaM}$ OSNs are the same as in wild type OSNs.

Collectively, these results suggest that Ca^{2+}/CaM-mediated fast desensitization through the B1b subunit of the CNG channel is not necessary for OSN adaptation to repeated stimulation.

CNGB1$^{\Delta CaM}$ OSNs display slower response termination

Rapid termination after the end of an odorant stimulus is a key feature of the OSN response. EOG recording revealed that CNGB1$^{\Delta CaM}$ OSNs, while having normal sensitivity and onset kinetics to 100 ms odorant exposures, displayed a clear deficit in the rate of response termination. This phenotype is shown in Figure 5A by superimposing amplitude-normalized and averaged EOG traces of wild type and CNGB1$^{\Delta CaM}$ mice to a 100 ms pulse of amyl acetate from vapor of a 10^{-4} M solution. The termination phase of these EOG signals was fit well with single exponential functions. The time constants of EOG decay for amyl acetate at 10^{-4}, 10^{-3}, and 10^{-2} M in CNGB1$^{\Delta CaM}$ OE were all significantly longer than their wild type counterparts (Figure 5B, Table 1).

The slower termination kinetics in CNGB1$^{\Delta CaM}$ OSNs was further confirmed at the single cell level. The currents of freshly dissociated OSNs were recorded using suction pipette electrodes and IBMX as the stimulant (Figure 5C). IBMX perfusion (1 mM, 1 second) induced similar peak currents in both genotypes (Figure 5D), but it took significantly longer for currents to decline to 20% of the end-perfusion value in CNGB1$^{\Delta CaM}$ OSNs than in wild type OSNs (Figure 5E).

Together, these results reveal that Ca^{2+}/CaM-mediated fast desensitization through the B1b subunit of the CNG channel accelerates response termination in OSNs.

Slowed response termination in CNGB1$^{\Delta CaM}$ OSN leads to loss of action potential generation in a paired-pulse paradigm

The slower termination of the suction current in CNGB1$^{\Delta CaM}$ OSNs might compromise the cell's ability to fire action potentials to subsequent stimulation. We proceeded to investigate the effect of the slower response termination on action potential firing. Figure 6 shows suction pipette currents of a wild type and a CNGB1$^{\Delta CaM}$ OSN in response to two 1-second exposures to 1 mM IBMX with a 0.25 second interpulse interval. Both cells fire action potentials during the rising phase of the suction current to the first exposure. In the wild type OSN, the suction current decayed quickly after the first exposure and the second exposure triggered a train of action potentials during the rising phase of the suction current. In contrast, the current to the first exposure in the CNGB1$^{\Delta CaM}$ OSN terminated more slowly, such that the current had not subsided at the end of the 0.25 second interpulse period and no action potential events were observed in response to the second exposure. Given that CNGB1$^{\Delta CaM}$ OSNs still generated an increase in suction current of similar size as the wild type, it is the slowed current decline that leads to a cessation of action potential firing, presumably due to continued inactivation of voltage-gated Na^+ channels (Trotier, 1994). At the short interpulse interval of 0.25 seconds, CNGB1$^{\Delta CaM}$ OSNs were significantly less likely to fire action potentials as compared to the wild type (16% of CNGB1$^{\Delta CaM}$ OSNs fired action potentials versus 47% of wild type OSNs. Figure 6, bottom panel and inset). The likelihood to fire action potentials was found to recover fully in both genotypes when the interpulse period was lengthened to 1 sec or longer.

CNGB1$^{\Delta CaM}$ mice displayed slower recovery of the odor-evoked local field potentials in the olfactory bulb in a paired-pulse paradigm

OSNs provide a direct excitatory input to a set of projection neurons (mitral/tufted cells) as well as an elaborate network of local neurons (juxtaglomerular cells) in the OB. The reduced ability of CNGB1$^{\Delta CaM}$ OSNs to fire action potentials to subsequent odor stimulation might result in altered activity of the OB neurons. To test this, we recorded local field potentials (LFPs), a measure of integrated electrical activity in the OB, of anesthetized wild type and CNGB1$^{\Delta CaM}$ mice. LFPs were recorded to a series of paired 200 ms odor pulses of amyl acetate. The two consecutive odor pulses were delivered at the same phase of the breathing cycle by triggering the olfactometer from the animal's breathing activity (Figure 7A and B). In the absence of odor, LFPs were highly correlated with the breathing cycles in both genotypes (Figure 7C and D). Odor presentation increased the amplitude of the LFP. In both wild type and CNGB1$^{\Delta CaM}$ mice, during short interstimulus intervals (ISI) the LFP amplitude to the second odor pulse was reduced compared to the initial response. As the ISI lengthened, the LFP amplitude to the second odor pulse recovered. The time course of LFP recovery in CNGB1$^{\Delta CaM}$ mice was slower compared to wild type mice (the time constant of LFP recovery in wild type, 0.35±0.042 sec; in CNGB1$^{\Delta CaM}$, 0.50±0.048 sec. N=5, p=0.045) (Figure 7E and F).

These data suggested that the reduced ability of CNGB1$^{\Delta CaM}$ OSN to fire action potentials during the short recovery period (Figure 6) likely results in reduced activation of their postsynaptic partners. Therefore, the termination deficit in receptor current of CNGB1$^{\Delta CaM}$ OSNs could transmit through the OB and affect central processing of olfactory information.

CNGB1$^{\Delta CaM}$ OSNs exhibit reduced adaptation during sustained stimulation

We further examined how elimination of Ca^{2+}/CaM-mediated fast desensitization of the CNG channel affects the OSN response to sustained odor exposure. Figure 8A shows EOG signals of wild type and CNGB1$^{\Delta CaM}$ mice to a 20-second odorant pulse from the vapor of a 10^{-4} M amyl acetate solution. In the wild type OE, the EOG amplitude declined progressively during the stimulation with a time constant of 3.13±0.38 second (mean±SD, n=6 mice) (see figure legend for note). In the CNGB1$^{\Delta CaM}$ OE, the EOG amplitude also exhibited a significant

reduction, but at a rate two fold slower (τ=6.22±1.12 second, n=6), suggesting that Ca^{2+}/CaM-mediated CNG channel desensitization contributes to OSN adaptation during sustained odorant stimulation (Figure 8B). In CNGB1$^{\Delta CaM}$ mice, sustained stimulation also caused a longer EOG rise time than in wild type mice (Figure 8C). The averaged peak amplitudes of the two genotypes were not significantly different.

Corroborative results were obtained from single cells recordings. As shown in Figure 6C, when stimulated with IBMX (1 mM, 1 second) both wild type and CNGB1$^{\Delta CaM}$ receptor currents declined after reaching their peak during the 1-second stimulation period. Significantly larger currents were recorded at the end of the stimulation in CNGB1$^{\Delta CaM}$ OSNs compared to wild type, suggesting attenuated adaptation (Figure 5F). While peak currents are not significantly different between the two genotypes (Figure 5D), the time to peak is delayed in CNGB1$^{\Delta CaM}$ OSNs (Figure 5G). Also, during prolonged stimulation, mouse OSNs display an oscillatory response pattern (Reisert & Matthews 2001), the frequency of which remained unaltered in CNGB1$^{\Delta CaM}$ OSNs (Supplemental Data Figure S2), contrary to a modeling study (Reidl et al., 2006) which suggested that the Ca^{2+}/CaM feedback desensitization of CNG channel alone can generate the observed oscillations.

Discussion

In this study, we conducted *in vivo* "loss-of-function" experiments to examine the role of Ca^{2+}/CaM-mediated olfactory CNG channel desensitization in regulation of OSN responses. In OSNs, this negative feedback mechanism has been previously inferred to be the dominant mechanism responsible for adaptation to repeated stimulation (Boccaccio et al., 2006; Kurahashi and Menini, 1997; Munger et al., 2001). We introduced a mutation in the CNGB1b channel subunit in mice and showed this mutation rendered the olfactory CNG channel resistant to desensitization by Ca^{2+}/CaM. We also showed that the protein expression, the cilial localization, and the cAMP sensitivity of the mutant channel were not affected by the mutation. With these points in mind, any physiological defect can be attributed to the loss of channel desensitization by Ca^{2+}/CaM. Contrary to expectations, our data showed that in CNGB1$^{\Delta CaM}$ mice the mutant OSNs had normal adaptation when peak EOG and suction current responses were examined in repeated stimulation paradigms, despite the lack of Ca^{2+}/CaM desensitization of the CNG channel. The mutant OSNs instead displayed a slower rate of response termination as well as attenuated adaptation during sustained odorant exposure. These results suggest that Ca^{2+}/CaM-mediated fast desensitization of the CNG channel plays a less important role in regulating response amplitudes to recurring stimulation than previously thought and instead functions primarily to terminate the OSN response during and after stimulation.

Rapid termination of the odorant-induced receptor potential is crucial for transmitting olfactory information regarding closely-occurring stimulations to the OB, as CNGB1$^{\Delta CaM}$ mice show slower recovery of OSN action potential generation and OB activity following an initial odor exposure.

Ca^{2+}/CaM-mediated CNG channel desensitization is not necessary for decreasing OSN responses to recurring stimulations

Adaptation is a common feature of sensory transduction. In OSNs, Ca^{2+} has been demonstrated to play a central role in mediating cellular adaptation by potentially modulating several signal transduction proteins via CaM (Kurahashi and Shibuya, 1990; Leinders-Zufall et al., 1998). Ca^{2+} that enters the cilium through CNG channels binds to CaM and can potentially decrease OSN sensitivity in at least three ways: first, by desensitizing the olfactory CNG channel; second, by stimulating a Ca^{2+}/CaM-dependent phosphodiesterase, PDE1C, leading to increased cAMP degradation (Yan et al., 1995); and third, by triggering inhibition of ACIII

activity via Ca^{2+}/CaM-dependent protein kinase II, which antagonizes cAMP synthesis (Leinders-Zufall et al., 1999; Wei et al., 1998). Ca^{2+}-independent mechanisms including inhibition of ACIII activity by a regulator of G-protein signaling protein, RGS2 (Sinnarajah et al., 2001), potentiation of G_{olf} activity by a GTP exchange factor, Ric-8b (Von Dannecker et al., 2005), and odorant receptor phosphorylation (Dawson et al., 1993; Schleicher et al., 1993) have also been suggested to contribute to OSN adaptation.

Although the relative involvement of any above mechanisms remains unknown, it has nevertheless been inferred from two lines of investigations that Ca^{2+}/calmodulin-mediated CNG channel desensitization serves as the dominant mechanism for OSN adaptation to repeated stimuli. First, intracellular pulses of cAMP or non-hydrolysable cAMP analogues produced by photolysis of caged-cyclic nucleotides caused similar adaptation to odorant stimulation in paired-pulse paradigms (Boccaccio et al., 2006; Kurahashi and Menini, 1997). Since the artificial cyclic nucleotide pulses bypassed odorant-stimulated cAMP production steps and non-hydrolysable cAMP analogues eliminated the influence of PDE, the mechanism that causes OSN adaptation was attributed to Ca^{2+}/CaM-mediated feedback desensitization of the CNG channel. These experiments, however, did not provide direct evidence that the desensitization of the channel via CaM underlies adaptation and also could not answer whether CNG channel desensitization is necessary for adaptation. Second, knockout of the CNGA4 subunit resulted in an elimination of OSN adaptation tested with paired-pulse paradigms and also a significant adaptation deficit tested with sustained stimulation (Munger et al., 2001). These phenotypes were attributed to the lack of Ca^{2+}/CaM-mediated CNG channel fast desensitization because the CNG channel from CNGA4$^{-/-}$ OSNs (presumably A2/B1b heteromers) exhibited only slow desensitization by Ca^{2+}/CaM. However, the loss of CNGA4 changes the subunit composition of the channel, causes reduced channel trafficking to the cilia (Michalakis et al., 2006), decreases the sensitivity of the channel to cAMP, and decreases the magnitude of OSN responses to odorants (Munger et al., 2001). A similar situation occurs in CNGB1 knockout (Michalakis et al., 2006). It is possible that because of the reduced OSN sensitivity, the apparent adaptation deficit in CNGA4$^{-/-}$ OSNs stems from recruitment of fewer adaptation mechanisms by the initial stimulus than in wild type cells.

Our data showed that CNGB1$^{\Delta CaM}$ OSNs displayed similarly decreased response amplitude of EOG and suction current to the second stimulus in a paired-pulse paradigm as compared to the wild type. The normal adaptation was seen with interpulse intervals as short as 1 second in EOG experiments and 0.25 seconds in single cell experiments (Figure 4). The mutated channel exhibited only a slow desensitization by Ca^{2+}/CaM (97 seconds time constant in mutant channels vs. 0.78 seconds in wild type). Other CaM-binding domains in A2 and A4 subunits may be responsible for this remaining slow desensitization. The very slow desensitization kinetics of the mutant channel is unlikely to account for OSN adaptation seen in our experimental time frame. These results demonstrate that desensitization of the CNG channel by Ca^{2+}/CaM is not necessary for decreasing OSN response to a recurring odorant stimulus. Mechanisms that regulate other components of the signal transduction pathway including Ca^{2+}/CaM-mediated regulation of PDE1C and ACIII are likely to underlie OSN adaptation to repeated stimulation. Feedback desensitization of the CNG channel via calcium-dependent protein(s) other than CaM (Balasubramanian et al., 1996;Hackos and Korenbrot, 1997;Rebrik and Korenbrot, 1998) could also account for the normal adaptation seen in CNGB1$^{\Delta CaM}$ OSNs, but the molecular identity of this potential inhibitor remains speculative.

Ca^{2+}/CaM-mediated CNG channel desensitization acts as a termination mechanism for shaping OSN responses during and after stimulation

The amplitude and shape of OSN responses can be envisioned as the result of a tug-of-war between activation and termination mechanisms. Our data establish that Ca^{2+}/CaM-mediated

fast desensitization of the CNG channel acts as a termination mechanism to shape OSN responses during and after stimulation. The lack of this termination mechanism in CNGB1$^{\Delta CaM}$ OSNs results in slower response termination and also in a longer response rise time and reduced response decline during sustained stimulation.

Our data reveal that Ca^{2+}/CaM-mediated fast desensitization of the CNG channel makes an essential contribution to rapid termination of OSN response. The slower termination kinetics observed in CNGB1$^{\Delta CaM}$ OSNs (Figure 5) are consistent with the idea that mutant CNG channels retain higher sensitivity to cAMP at the end of a stimulation compared to desensitized channels in the wild type OSN, so more channels can remain open in CNGB1$^{\Delta CaM}$ OSNs during the decrease of cilial cAMP after the stimulation. In addition to Ca^{2+}/CaM-mediated CNG channel desensitization, two other mechanisms have been previously suggested to also contribute to rapid termination of OSN electrical responses. One is the degradation of cAMP by phosphodiesterase activity that leads to the closure of the CNG channel (Firestein et al., 1991). PDE1C has been specifically located in the cilia (Juilfs et al., 1997) and is likely responsible for the degradation of cilial cAMP (Borisy et al., 1992). The other is the extrusion of cilial calcium by Na^+/Ca^{2+} exchangers (Reisert and Matthews, 1998) that leads to the closure of the Ca^{2+}-activated Cl^-channel. These mechanisms likely work in concert to ensure the OSN response terminates rapidly after stimulation.

Rapid termination of the stimulus-induced receptor potential is thought to enable OSNs to recover sufficiently to fire action potentials to subsequent stimulation. Prolonged depolarization can reduce the neuron's ability to fire action potentials to subsequent stimulation due to inactivation of voltage-gated Na^+ channels. Consistent with this idea, CNGB1$^{\Delta CaM}$ OSNs showed a reduced ability to fire action potentials in response to the second stimulation of a paired-pulse stimulation paradigm at short interpulse interval, as compared to wild type (Figure 6), even though the amplitude of the suction current elicited by the second stimulation is similar to the wild type. Such a physiological deficit alters the input to the OB. Indeed, in a paired-pulse paradigm, the odor-evoked local field potentials recorded from a deep position in the OB displayed slower recovery of the amplitude to the second pulse in CNGB1$^{\Delta CaM}$ mice as compared to the wild type (Figure 7). These findings suggest that the phenotype observed in the OSNs is transmitted through the OB and is likely to affect central processing of olfactory information, thus compromising the animal's behaviors that require fast temporal resolution of olfactory information.

When responding to brief odorant pulses (100 ms), the EOG amplitude and the signal rise time were not significantly different between wild type and CNGB1$^{\Delta CaM}$ OSNs (Table 1), implying that the extent of channel desensitization is not sufficient to significantly influence the amplitude and activation kinetics, although in wild type OSNs the channel desensitization must begin before the peak time because the termination deficit was instantly apparent in CNGB1$^{\Delta CaM}$ OSNs following the peak of the response. The rise time to brief odorant stimulation is likely to be determined primarily by the shutoff of activation mechanisms due to the end of stimulation. When responding to longer stimuli, the influence of the Ca^{2+}/CaM-mediated CNG channel desensitization on the rise time becomes evident. In wild type OSNs, the channel desensitization together with other termination mechanisms progressively surpasses ongoing activation mechanisms such that the response reaches a peak and begins to decline. The lack of this termination mechanism in CNGB1$^{\Delta CaM}$ OSNs causes the EOG signal to peak at a delayed time (Figure 8A, C).

Ca^{2+}/CaM-mediated CNG channel desensitization affects not only the time at which the response decline begins but also the rate and the level of the response decline during sustained odorant exposure. The response decline during sustained stimulation is defined as a form of adaptation. CNGB1$^{\Delta CaM}$ OSNs showed reduced response decline during sustained odorant

exposure (Figure 8A, B), suggesting that Ca^{2+}/CaM desensitization of the CNG channel contributes to this form of adaptation. The reduced response decline in CNGB1$^{\Delta CaM}$ OSNs is again consistent with the concept that the mutant CNG channel retains higher sensitivity to cAMP during the period of sustained stimulation compared to desensitized channels in the wild type OSN. However, the role of the channel desensitization in OSN adaptation during the sustained stimulation is partial, as CNGB1$^{\Delta CaM}$ OSNs still retain significant response reductions.

Beyond OSNs

The CNGB1 gene is expressed as an alternatively spliced form, CNGB1a, in rod photoreceptors in the visual system (Korschen et al., 1995; Sautter et al., 1998). The rod CNG channel, composed of the CNGA1 and CNGB1 subunits, is also subject to desensitization by Ca^{2+}/CaM (Gordon et al., 1995; Hsu and Molday, 1993). The rod CNG channel of the CNGB1$^{\Delta CaM}$ mouse is expected to be insensitive to the Ca^{2+}/CaM as the CNGA1 subunit does not contain any CaM-binding domain (Trudeau and Zagotta, 2003). The CNGB1$^{\Delta CaM}$ mouse provides an animal model to address the physiological significance of Ca^{2+}/CaM-mediated desensitization of the rod CNG channel in regulation of rod phototransduction. In addition, many other calcium permeable ion channels including voltage gated calcium channels (Liang et al., 2003) and NMDA glutamate receptors (Ehlers et al., 1996) are subject to negative feedback regulation by Ca^{2+} via calmodulin. A similar strategy should be applicable to study the physiological significance of such modulation to these calcium permeable channels.

Experimental Procedures

For all experiments, mice were handled and euthanized with methods approved by the Animal Care and Use Committees of each applicable institution. Additional details on experimental procedures are included in Supplemental Data.

Generation of CNGB1$^{\Delta CaM}$ mice

The coding sequence for the N-terminal CaM-binding domain of CNGB1 lies in a single exon. The targeting vector consists of 5' (5.2 kb) and 3' (4.9 kb) arms and an insertion fragment, which contains a modified exon missing the coding sequence for LQELVKMFKERTEKVKEKLI and a loxP-neo-loxP (LNL) selection cassette. The LNL selection cassette is inserted into the intron that follows the CaM-binding domain coding exon. Homologous recombination events in ES cells were screened by PCR of genomic DNA and confirmed by Southern blot. Blastocyst injection of the modified ES cells was done at the Johns Hopkins University transgenic facility. The LNL fragment was removed from the genome by mating the F1 heterozygotes with cre-transgenic mice.

Molecular characterization of CNG channel subunit expressions

Immunohistochemistry: Olfactory tissues were fixed with 4% paraformaldehyde. Cryosections (14 μm) were cut and incubated overnight with primary antibodies at 4°C, followed by incubation with fluorescent secondary antibodies and imaging by confocal microscopy. Western blot: OE tissue was homogenized in 2X Laemmli buffer followed by SDS-PAGE. The blot was blocked with 5% non-fat dry milk and incubated overnight with primary antibodies at 4°C. Following incubation with HRP-linked secondary antibodies, the blot was treated with ECL Plus regent (Amersham) and exposed to film.

Electroolfactogram

EOG recording was performed as described (Zhao et al., 1998). The head of an euthanized mouse was cut sagittally to expose the medial surface of the olfactory turbinates. The EOG

signals were recorded from location 1 as marked in Figure 3A unless otherwise noted. The signals were acquired and analyzed with AxoGraph software (Axon Instruments). The signals were recorded at a sampling rate of 1KHz and low-pass filtered at 25 Hz when analyzed. Vapor-phase odorant stimuli are generated by placing 5 ml of odorant solution in a sealed 60 ml glass bottle. This vapor is delivered as a pulse injected into a continuous stream of humidified air flowing over the tissue. All EOG recordings were conducted at room temperature and in mice older than 6 weeks.

Single cell and excised patch recordings

Suction pipette recordings were performed as described (Reisert and Matthews, 2001). The cell body of an isolated OSN was sucked into the tip of the recording pipette leaving the cilia exposed to the bath solution and accessible for solution changes. Experiments were performed at 37°C.

For excised patch experiments olfactory tissue was dissociated as described (Reisert et al., 2003). Inside-out patches were excised from dendritic knobs of OSNs. Often cilia were visible and could be sucked into the recording pipette before sealing. The open-pipette resistance of the patch pipette was 7-8 MΩ. The holding potential was –40 mV. Most experiments were performed in 140 mM symmetrical NaCl solution, with 10 mM HEPES and 10 mM HEDTA. Adding 9.98 mM $CaCl_2$ yielded a free Ca^{2+} concentration of 67 μM. The inhibition of the CNG channel by Ca^{2+}/calmodulin was investigated in a solution where 130 mM NaCl were replaced equimolarly by sodium methanesulfonate to minimize the Ca^{2+}-activated Cl^- current. 5 mM nitrilotriacetic acid (NTA) and 1.87 mM $CaCl_2$ were added to solutions to contain 100 μM free Ca^{2+}. Also 1 mM niflumic acid was added to the pipette solution to suppress the remaining Cl^- current. All solutions contained 10 mM HEPES, the pH was adjusted to 7.2 with NMDG.

Solution exchanges were applied by transferring the tip of the recording pipette across the interface of neighboring streams of solution using the Perfusion Fast-Step SF-77B solution changer (Warner Instruments). Currents were recorded with a Warner PC-501A patch clamp amplifier, digitized using a Mikro1401 and Signal acquisition software (Cambridge Electronic Design, U.K.). Excised patch recordings were sampled at 2 KHz and low-pass-filtered at 100 Hz. All odorant-induced suction currents were sampled at 10 KHz and filtered DC-50 Hz to display the suction current. Only the traces in Figure 6 were filtered DC-5000 Hz to investigate action potential firing.

The analysis for the action potential firing during the paired-pulse paradigm was conducted as follows: For each cell and each interpulse interval a “1” or a “0” was attributed when action potentials were or were not observed in response to the second stimulation. For each genotype, the percentage of OSNs firing action potentials for a given interpulse interval was calculated. Each sweep was regarded as a Bernoulli trial and the variance was calculated as p*(1-p) with p being the average of each interpulse interval (Rosner, 2006).

Olfactory bulb field potential recordings

Mice anesthetized with ketamine/xylazine were mounted in a stereotaxic frame with body temperature maintained at 37°C. The animal’s nose was inserted into an airtight gas mask through which humidified air from the olfactometer passed at a rate of 1 liter/min. A custom-made olfactometer was adapted from a previous design (Lorig et al., 1999). The odorant amyl acetate was dissolved in 1 ml DMSO at 0.5 mM, and a 20 ml vapor headspace was kept saturated with a cotton or paper wick to maximize liquid surface area. For each mouse, a series of paired odor pulses (0.2 sec each) at varying interstimulation intervals (ISIs) (~0.3 to ~10 sec) was delivered at least 5 times separated with pulses of solvent headspace. The paired pulses were

delivered at the same phase of the breathing cycle. This was achieved by triggering the olfactometer from a piezoelectric sensor attached to the animals' chest.

A small craniotomy was performed at the left hemisphere corresponding to the central dorsal surface of the main OB. A tungsten electrode with an impedance of 0.7-2 MΩ was inserted ~1 mm deep into the bulb (granule cell layer). Recording from deep layer of the bulb with low impedance electrode avoids location bias. In some animals the position of the recording electrode was confirmed histologically after burning the tip position, and visualized in 100 μm vibrotome slices with cresyl violet. LFPs were amplified, filtered (1 Hz highpass, 3 KHz lowpass), and digitized at 5-10 KHz. All on-line event detection, triggering and off-line analysis was done using the software Spike2 (CED, UK).

Supplementary Material

Refer to Web version on PubMed Central for supplementary material.

Acknowledgements

We thank Dr. Joseph Beavo for PDE1C antibody, Drs. Wei Chen, Carter Cornwall, Douglas Fambrough, Stuart Firestein, Alan Gelperin, Ali Guler, Samer Hattar, Rejji Kuruvilla, Graeme Lowe, Minmin Luo, Minghong Ma, Randall Reed and the anonymous reviewers for suggestions and comments on experiments and the manuscript, Dr Paul Breslin and Greg Shaffer for advice on statistics and members of the Hattar-Kuruvilla-Zhao mouse tri-lab of the Department of Biology, Johns Hopkins University for discussion. Supported by the Whitehall Foundation, NIH DC006178, and the Monell Chemical Senses Center.

References

Balasubramanian S, Lynch JW, Barry PH. Calcium-dependent modulation of the agonist affinity of the mammalian olfactory cyclic nucleotide-gated channel by calmodulin and a novel endogenous factor. J Membr Biol 1996;152:13–23. [PubMed: 8660407]

Boccaccio A, Lagostena L, Hagen V, Menini A. Fast adaptation in mouse olfactory sensory neurons does not require the activity of phosphodiesterase. J Gen Physiol 2006;128:171–184. [PubMed: 16880265]

Bonigk W, Bradley J, Muller F, Sesti F, Boekhoff I, Ronnett GV, Kaupp UB, Frings S. The native rat olfactory cyclic nucleotide-gated channel is composed of three distinct subunits. J Neurosci 1999;19:5332–5347. [PubMed: 10377344]

Borisy FF, Ronnett GV, Cunningham AM, Juilfs D, Beavo J, Snyder SH. Calcium/calmodulin-activated phosphodiesterase expressed in olfactory receptor neurons. J Neurosci 1992;12:915–923. [PubMed: 1312138]

Bradley J, Bonigk W, Yau KW, Frings S. Calmodulin permanently associates with rat olfactory CNG channels under native conditions. Nat Neurosci 2004;7:705–710. [PubMed: 15195096]

Chen TY, Yau KW. Direct modulation by Ca(2+)-calmodulin of cyclic nucleotide-activated channel of rat olfactory receptor neurons. Nature 1994;368:545–548. [PubMed: 7511217]

Dawson TM, Arriza JL, Jaworsky DE, Borisy FF, Attramadal H, Lefkowitz RJ, Ronnett GV. Beta-adrenergic receptor kinase-2 and beta-arrestin-2 as mediators of odorant-induced desensitization. Science 1993;259:825–829. [PubMed: 8381559]

Ehlers MD, Zhang S, Bernhadt JP, Huganir RL. Inactivation of NMDA receptors by direct interaction of calmodulin with the NR1 subunit. Cell 1996;84:745–755. [PubMed: 8625412]

Firestein S. How the olfactory system makes sense of scents. Nature 2001;413:211–218. [PubMed: 11557990]

Firestein S, Darrow B, Shepherd GM. Activation of the sensory current in salamander olfactory receptor neurons depends on a G protein-mediated cAMP second messenger system. Neuron 1991;6:825–835. [PubMed: 1709025]

Gordon SE, Downing-Park J, Zimmerman AL. Modulation of the cGMP-gated ion channel in frog rods by calmodulin and an endogenous inhibitory factor. J Physiol 1995;486(Pt 3):533–546. [PubMed: 7473217]

Grunwald ME, Yu WP, Yu HH, Yau KW. Identification of a domain on the beta-subunit of the rod cGMP-gated cation channel that mediates inhibition by calcium-calmodulin. J Biol Chem 1998;273:9148–9157. [PubMed: 9535905]

Hackos DH, Korenbrot JI. Calcium modulation of ligand affinity in the cyclic GMP-gated ion channels of cone photoreceptors. J Gen Physiol 1997;110:515–528. [PubMed: 9348324]

Hsu YT, Molday RS. Modulation of the cGMP-gated channel of rod photoreceptor cells by calmodulin. Nature 1993;361:76–79. [PubMed: 7678445]

Juilfs DM, Fulle HJ, Zhao AZ, Houslay MD, Garbers DL, Beavo JA. A subset of olfactory neurons that selectively express cGMP-stimulated phosphodiesterase (PDE2) and guanylyl cyclase-D define a unique olfactory signal transduction pathway. Proc Natl Acad Sci U S A 1997;94:3388–3395. [PubMed: 9096404]

Kaupp UB, Seifert R. Cyclic nucleotide-gated ion channels. Physiol Rev 2002;82:769–824. [PubMed: 12087135]

Kleene SJ. Origin of the chloride current in olfactory transduction. Neuron 1993;11:123–132. [PubMed: 8393322]

Korschen HG, Illing M, Seifert R, Sesti F, Williams A, Gotzes S, Colville C, Muller F, Dose A, Godde M, et al. A 240 kDa protein represents the complete beta subunit of the cyclic nucleotide-gated channel from rod photoreceptor. Neuron 1995;15:627–636. [PubMed: 7546742]

Kurahashi T, Menini A. Mechanism of odorant adaptation in the olfactory receptor cell. Nature 1997;385:725–729. [PubMed: 9034189]

Kurahashi T, Shibuya T. Ca2(+)-dependent adaptive properties in the solitary olfactory receptor cell of the newt. Brain Res 1990;515:261–268. [PubMed: 2113412]

Kurahashi T, Yau KW. Co-existence of cationic and chloride components in odorant-induced current of vertebrate olfactory receptor cells. Nature 1993;363:71–74. [PubMed: 7683113]

Leinders-Zufall T, Greer CA, Shepherd GM, Zufall F. Imaging odor-induced calcium transients in single olfactory cilia: specificity of activation and role in transduction. J Neurosci 1998;18:5630–5639. [PubMed: 9671654]

Leinders-Zufall T, Ma M, Zufall F. Impaired odor adaptation in olfactory receptor neurons after inhibition of Ca2+/calmodulin kinase II. J Neurosci 1999;19:RC19. [PubMed: 10407061]

Liang H, DeMaria CD, Erickson MG, Mori MX, Alseikhan BA, Yue DT. Unified mechanisms of Ca2+ regulation across the Ca2+ channel family. Neuron 2003;39:951–960. [PubMed: 12971895]

Liu M, Chen TY, Ahamed B, Li J, Yau KW. Calcium-calmodulin modulation of the olfactory cyclic nucleotide-gated cation channel. Science 1994;266:1348–1354. [PubMed: 7526466]

Lorig TS, Elmes DG, Zald DH, Pardo JV. A computer-controlled olfactometer for fMRI and electrophysiological studies of olfaction. Behav Res Methods Instrum Comput 1999;31:370–375. [PubMed: 10495824]

Lowe G, Gold GH. Nonlinear amplification by calcium-dependent chloride channels in olfactory receptor cells. Nature 1993;366:283–286. [PubMed: 8232590]

Michalakis S, Reisert J, Geiger H, Wetzel C, Zong X, Bradley J, Spehr M, Huttl S, Gerstner A, Pfeifer A, et al. Loss of CNGB1 protein leads to olfactory dysfunction and subciliary cyclic nucleotide-gated channel trapping. J Biol Chem 2006;281:35156–35166. [PubMed: 16980309]

Munger SD, Lane AP, Zhong H, Leinders-Zufall T, Yau KW, Zufall F, Reed RR. Central role of the CNGA4 channel subunit in Ca2+-calmodulin-dependent odor adaptation. Science 2001;294:2172–2175. [PubMed: 11739959]

Rebrik TI, Korenbrot JI. In intact cone photoreceptors, a Ca2+-dependent, diffusible factor modulates the cGMP-gated ion channels differently than in rods. J Gen Physiol 1998;112:537–548. [PubMed: 9806963]

Reidl J, Borowski P, Sensse A, Starke J, Zapotocky M, Eiswirth M. Model of calcium oscillations due to negative feedback in olfactory cilia. Biophys J 2006;90:1147–1155. [PubMed: 16326896]

Reisert J, Bauer PJ, Yau KW, Frings S. The Ca-activated Cl channel and its control in rat olfactory receptor neurons. J Gen Physiol 2003;122:349–363. [PubMed: 12939394]

Reisert J, Lai J, Yau KW, Bradley J. Mechanism of the excitatory Cl- response in mouse olfactory receptor neurons. Neuron 2005;45:553–561. [PubMed: 15721241]

Reisert J, Matthews HR. Na+-dependent Ca2+ extrusion governs response recovery in frog olfactory receptor cells. J Gen Physiol 1998;112:529–535. [PubMed: 9806962]

Reisert J, Matthews HR. Response properties of isolated mouse olfactory receptor cells. J Physiol 2001;530:113–122. [PubMed: 11136863]

Rosner, B. Fundamentals of biostatistics. 6. Belmont, CA: Thomson-Brooks/Cole; 2006.

Sautter A, Zong X, Hofmann F, Biel M. An isoform of the rod photoreceptor cyclic nucleotide-gated channel beta subunit expressed in olfactory neurons. Proc Natl Acad Sci U S A 1998;95:4696–4701. [PubMed: 9539801]

Schleicher S, Boekhoff I, Arriza J, Lefkowitz RJ, Breer H. A beta-adrenergic receptor kinase-like enzyme is involved in olfactory signal termination. Proc Natl Acad Sci U S A 1993;90:1420–1424. [PubMed: 8381966]

Schwenk F, Baron U, Rajewsky K. A cre-transgenic mouse strain for the ubiquitous deletion of loxP-flanked gene segments including deletion in germ cells. Nucleic Acids Res 1995;23:5080–5081. [PubMed: 8559668]

Scott JW, Scott-Johnson PE. The electroolfactogram: A review of its history and uses. Microsc Res Tech 2002;58:152–160. [PubMed: 12203693]

Sinnarajah S, Dessauer CW, Srikumar D, Chen J, Yuen J, Yilma S, Dennis JC, Morrison EE, Vodyanoy V, Kehrl JH. RGS2 regulates signal transduction in olfactory neurons by attenuating activation of adenylyl cyclase III. Nature 2001;409:1051–1055. [PubMed: 11234015]

Trotier D. Intensity coding in olfactory receptor cells. Semin Cell Biol 1994;5:47–54. [PubMed: 7514456]

Trudeau MC, Zagotta WN. Mechanism of calcium/calmodulin inhibition of rod cyclic nucleotide-gated channels. Proc Natl Acad Sci U S A 2002;99:8424–8429. [PubMed: 12048242]

Trudeau MC, Zagotta WN. Calcium/calmodulin modulation of olfactory and rod cyclic nucleotide-gated ion channels. J Biol Chem 2003;278:18705–18708. [PubMed: 12626507]

Von Dannecker LE, Mercadante AF, Malnic B. Ric-8B, an olfactory putative GTP exchange factor, amplifies signal transduction through the olfactory-specific G-protein Galphaolf. J Neurosci 2005;25:3793–3800. [PubMed: 15829631]

Wei J, Zhao AZ, Chan GC, Baker LP, Impey S, Beavo JA, Storm DR. Phosphorylation and inhibition of olfactory adenylyl cyclase by CaM kinase II in Neurons: a mechanism for attenuation of olfactory signals. Neuron 1998;21:495–504. [PubMed: 9768837]

Weitz D, Zoche M, Muller F, Beyermann M, Korschen HG, Kaupp UB, Koch KW. Calmodulin controls the rod photoreceptor CNG channel through an unconventional binding site in the N-terminus of the beta-subunit. Embo J 1998;17:2273–2284. [PubMed: 9545240]

Yan C, Zhao AZ, Bentley JK, Loughney K, Ferguson K, Beavo JA. Molecular cloning and characterization of a calmodulin-dependent phosphodiesterase enriched in olfactory sensory neurons. Proc Natl Acad Sci U S A 1995;92:9677–9681. [PubMed: 7568196]

Zhao H, Ivic L, Otaki JM, Hashimoto M, Mikoshiba K, Firestein S. Functional expression of a mammalian odorant receptor. Science 1998;279:237–242. [PubMed: 9422698]see comments

Zheng J, Zagotta WN. Stoichiometry and assembly of olfactory cyclic nucleotide-gated channels. Neuron 2004;42:411–421. [PubMed: 15134638]

Zufall F, Leinders-Zufall T. The cellular and molecular basis of odor adaptation. Chem Senses 2000;25:473–481. [PubMed: 10944513]

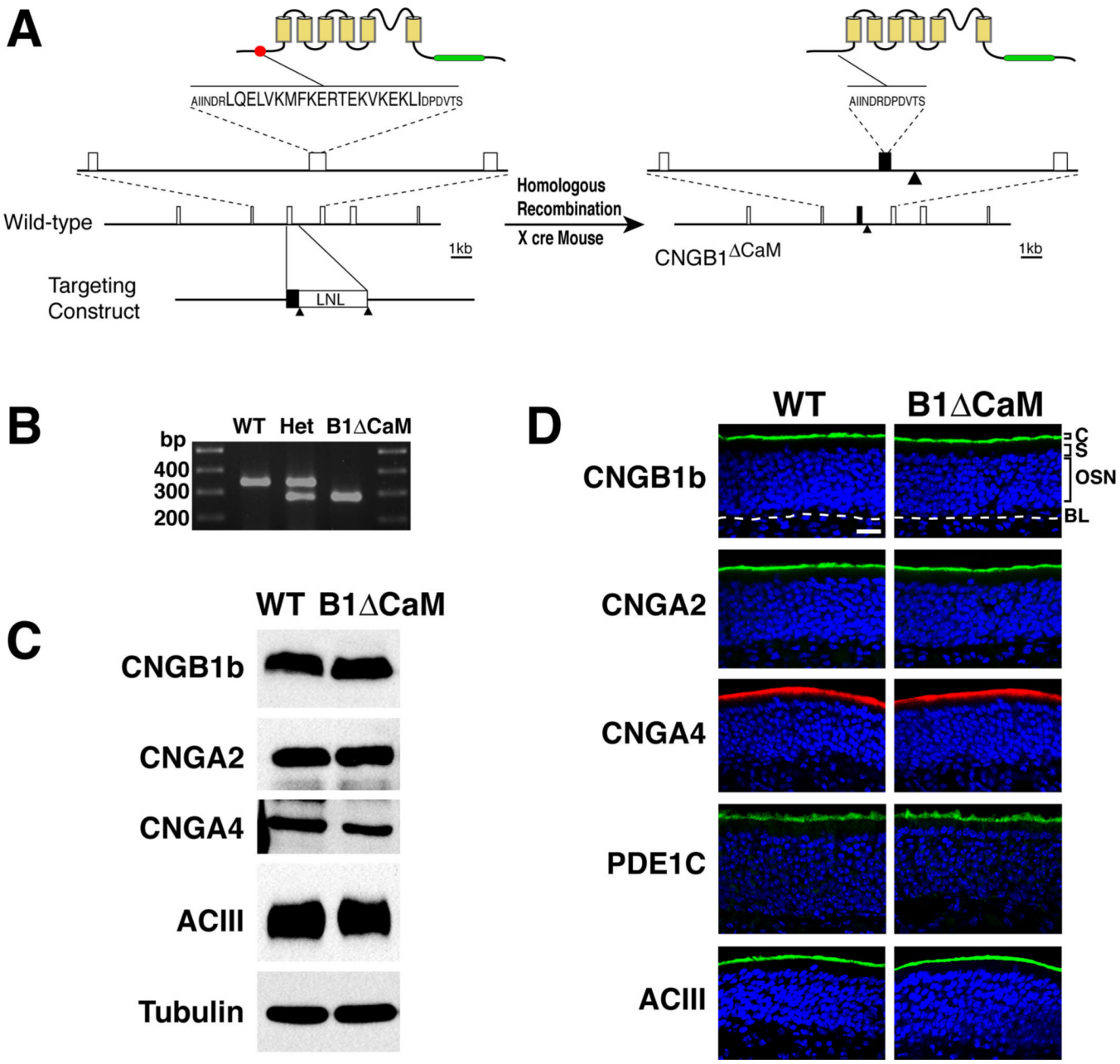

Figure 1. Generation and molecular characterization of CNGB1$^{\Delta CaM}$ mice

(A) Generation of CNGB1$^{\Delta CaM}$ mice. The left and the right panel are schematics of the CNGB1b protein structure and a portion of the *Cngb1* gene in the wild type and CNGB1$^{\Delta CaM}$ mice respectively. On the upper left, the N-terminal CaM-binding domain containing 20 amino acids in the CNGB1b protein is represented with a solid red circle. The transmembrane domains are depicted as yellow boxes and the cAMP-binding domain is represented as a green bar. Below, the exons of the *Cngb1* gene are shown as open boxes. The targeting construct is illustrated at the bottom. K, KpnI; H, HindIII; S, SpeI; Bs, BstEII; Solid triangles, loxP sites. On the right, the mutant CNGB1b protein lacks the CaM-binding domain. The mutated exon in the *Cngb1* gene is represented by the black box and the loxP site remaining in the intron is marked by the solid triangle.

(B) PCR analysis of genomic DNA across the deletion site. The precise elimination of the 60 nucleotides encoding 20 amino acid CaM-binding domain in the PCR products of CNGB1$^{\Delta CaM}$ mice were confirmed by sequencing.
(C) Western blot analysis of total OE proteins. CNGB1b, CNGA2, CNGA4, and ACIII are expressed at similar levels in wild type and CNGB1b$^{\Delta CaM}$ mice. α-tubulin is used as the loading control.
(D) Immunohistostaining of OE sections. CNGB1b, CNGA2, CNGA4, ACIII and PDE1C are all primarily detected at the cilial layer of the OE in both wild type and CNGB1b$^{\Delta CaM}$ mice. C, cilial layer; S, supporting cell layer; OSN, olfactory sensory neuron layer; BL, basal lamina, marked by a white dashed line. Scale bar: 20 μm.

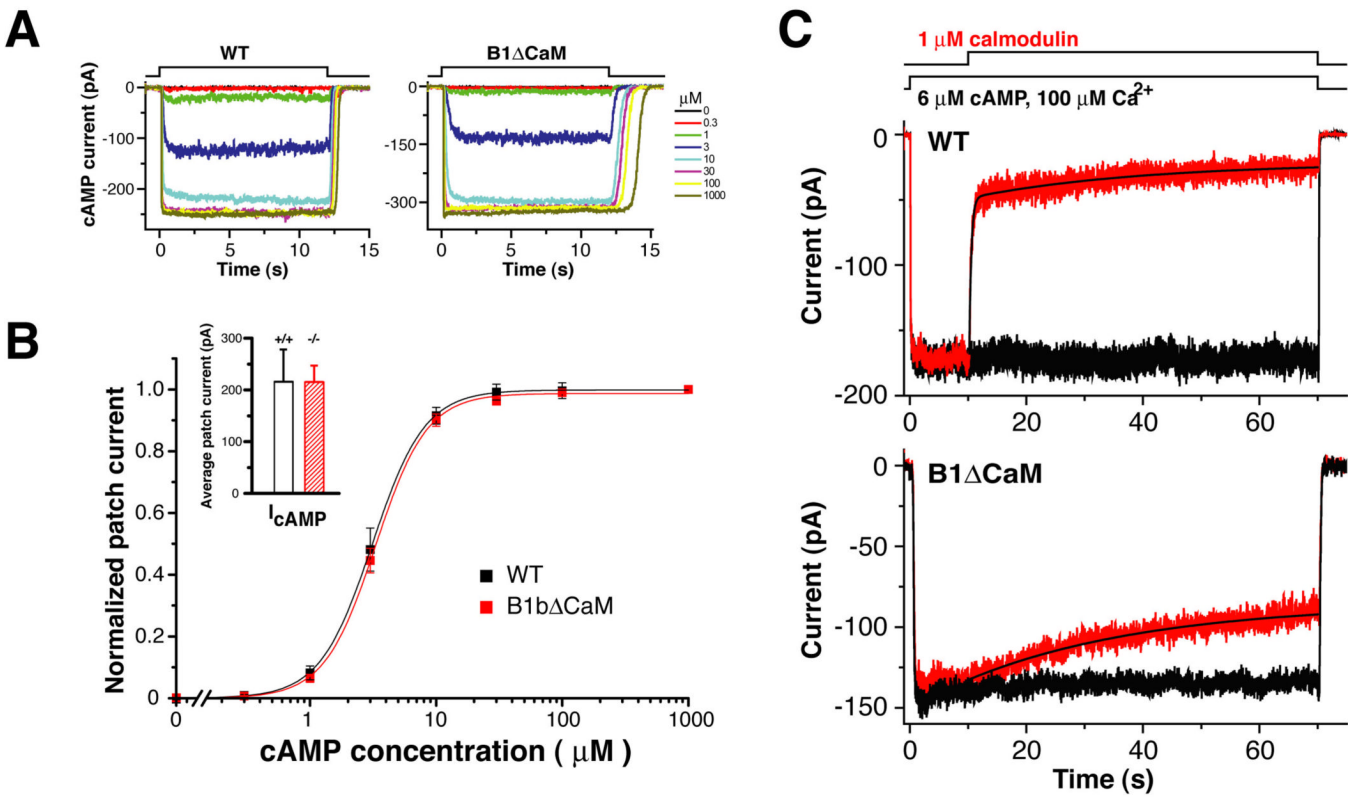

Figure 2. The CNG channel in CNGB1$^{\Delta CaM}$ OSNs has normal sensitivity to cAMP, but lacks fast desensitization by Ca^{2+}/CaM

(A) cAMP-induced currents of an inside-out excised membrane patch from the dendritic knob of a wild type OSN (left) and a CNGB1$^{\Delta CaM}$ OSN (right). Patches were perfused with increasing concentrations of cAMP.

(B) cAMP dose-response relations of the wild type and CNGB1$^{\Delta CaM}$ channels. Current values were obtained by averaging from a time point when a steady state was reached (typically 0.5 - 1 second) to the end of cAMP exposure (12 seconds). Solid lines represent Hill curves fitted to the data. The wild type and CNGB1$^{\Delta CaM}$ channels have virtually identical cAMP dose-response relations. Wild type channel $K_{1/2}$, 3.11±0.02 μM (mean±SEM, n=7); CNGB1$^{\Delta CaM}$ channel $K_{1/2}$, 3.30±0.07 μM (n=7). Inset, the averaged steady-state currents induced by a saturating concentration of cAMP (100 μM). Wild type, 216±62 pA (mean±SEM, n=8); CNGB1$^{\Delta CaM}$, 215±41 pA (n=20).

(C) Patches excised from wild type (upper panel) and CNGB1$^{\Delta CaM}$ (lower panel) OSNs were exposed to 6 μM of cAMP (the concentration corresponding to 0.75 open probability). The black trace represents the current evoked by cAMP in the absence of CaM. Application of CaM (red traces) quickly reduced the CNG current in patches from wild type OSNs, while causing only a slow reduction in patches from CNGB1$^{\Delta CaM}$ OSNs. The decay in wild type patches could be fitted with paired exponentials with average time constants of 0.78±0.42 seconds for the fast phase and 37±15 seconds (mean±SEM, n=4) for the slow phase. In CNGB1$^{\Delta CaM}$ patches, only a single exponential was fitted with an average time constant of 97±60 seconds (n=4). All experiments were performed in symmetrical Na-methanesulfonate solution (see Methods), and the pipette solution contained 1 mM niflumic acid to suppress the Ca^{2+}-activated Cl^- current.

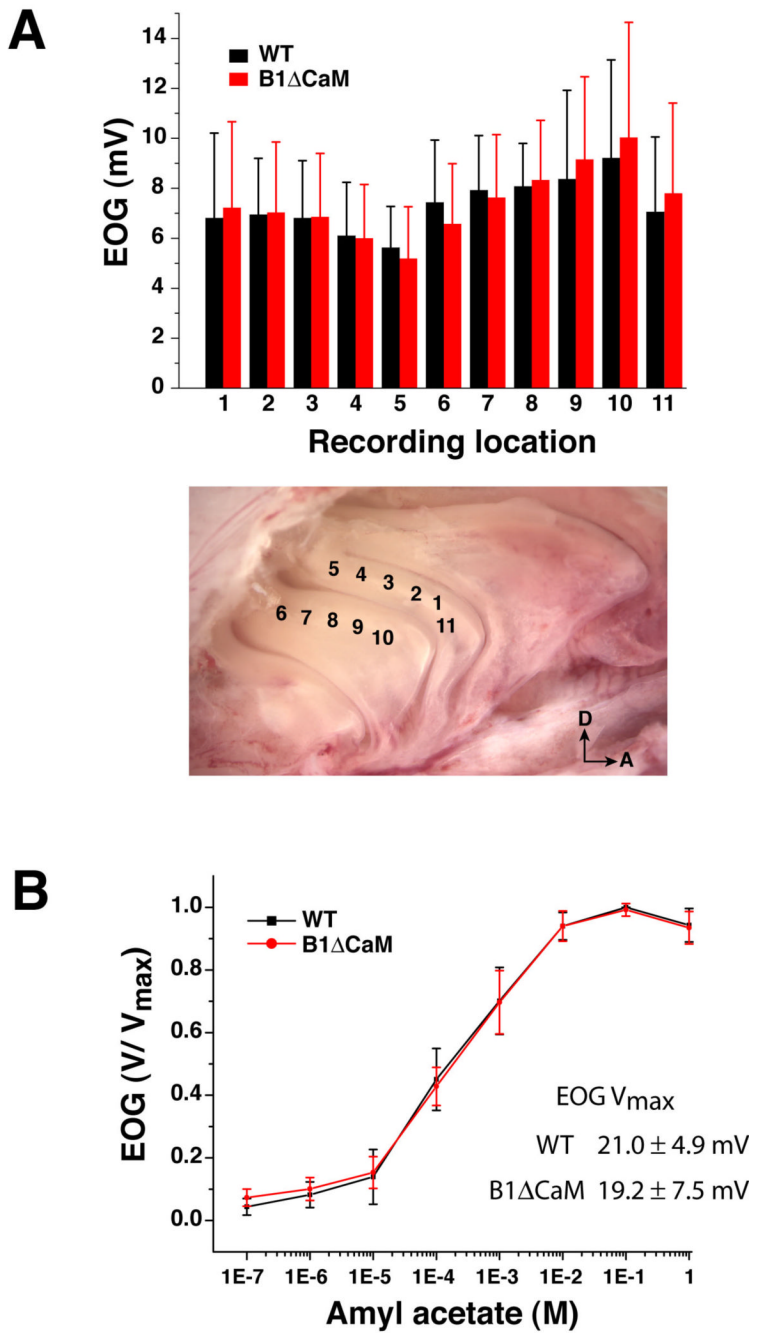

Figure 3. CNGB1$^{\Delta CaM}$ OSNs show normal sensitivity to initial odor stimulation

(A) Averaged EOG amplitudes (n=6 mice, error bars represent SD) to a 100 ms pulse of vapor of a bottle containing 10^{-4} M amyl acetate solution from eleven different locations along turbinate IIb and III. These locations are indicated in the photograph. D, dorsal; A, anterior. (B) Dose-response relations for amyl acetate. The epithelium was exposed to 100 ms pulses of vapor of increasing concentration of amyl acetate solution. The concentrations marked on the X-axis are the solution concentrations in the bottle. The data points (n=6 mice, error bars represent SD) are linked with straight line. The EOG signals were recorded from location 1.

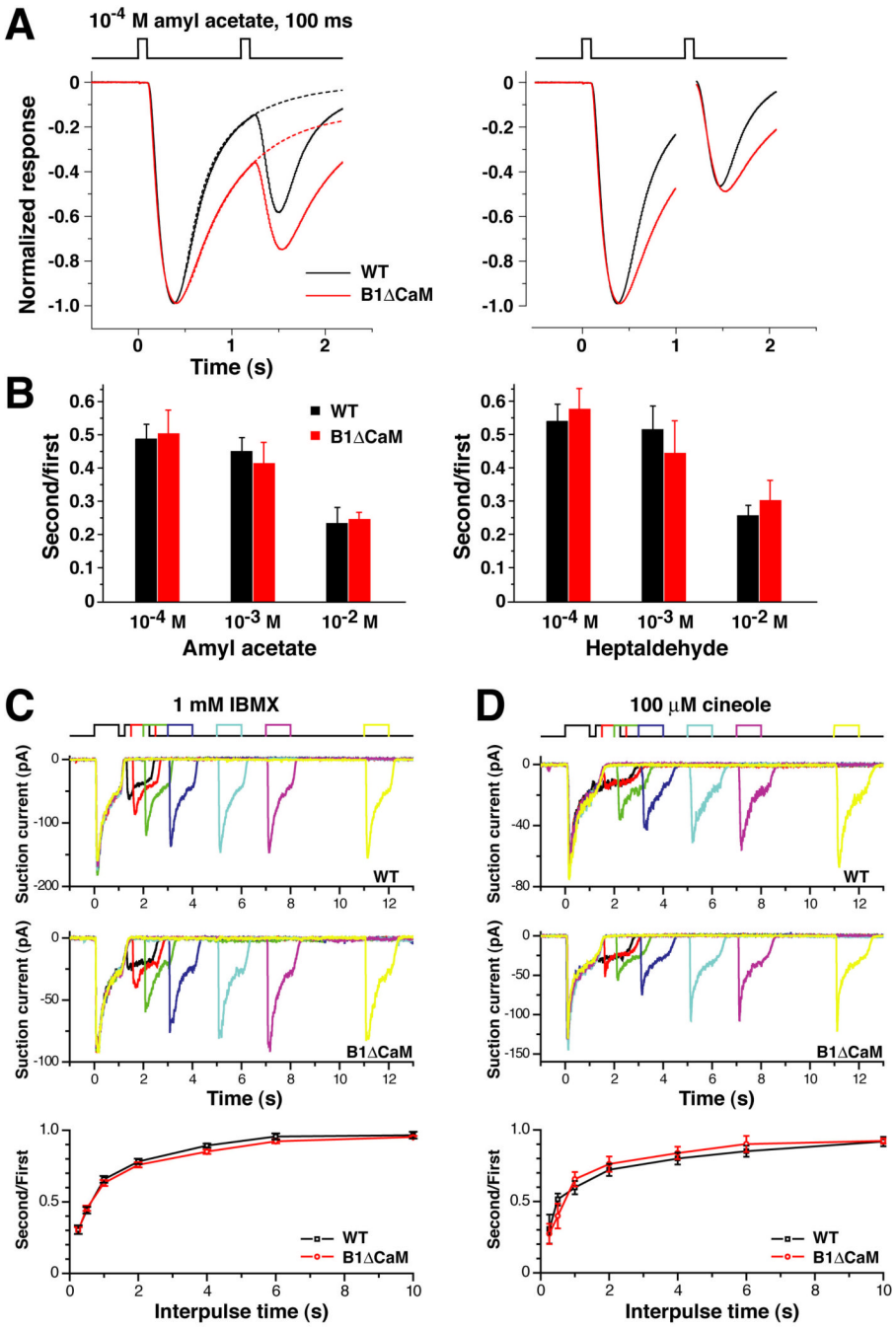

Figure 4. CNGB1$^{\Delta CaM}$ OSNs exhibit normal adaptation to repeated odor exposure

(A and B) EOG analysis.

(A) Left panel: Normalized EOG signals to two consecutive 100 ms pulses of vapor of 10^{-4} M amyl acetate solution with 1-second interpulse intervals. The traces of the wild type (black) and CNGB1$^{\Delta CaM}$ (red) mice, each the average from 6 animals, are superimposed. The dashed lines represent traces obtained by fitting the termination phase with a single exponential equation. Right panel: traces represent the averaged "net" response to each stimulus. Since the responses have not returned to the baseline when the second stimulus is given, for each recording the "net" response caused by the second stimulus is calculated by subtracting the

trace obtained by fitting the termination phase of the first response (illustrated by the dashed line in the left panel) from the trace of the second pulse.
(B) The net peak response ratios for amyl acetate (left) and heptaldehyde (right). CNGB1$^{\Delta CaM}$ OSNs exhibit comparable extent of adaptation to the wild type OSNs.
(C and D) Single cell analysis.
(C) Suction electrode recordings from an isolated wild type or CNGB1$^{\Delta CaM}$ OSN exposed twice to IBMX (1 mM, 1 second) with increasing interpulse intervals. Bottom panel: the ratios of the peak responses (second/first) are plotted against the interpulse time. Each data point is the average of 20 – 54 experiments, error bars represent SEM.
(D) Same experimental paradigm as in (C), but responses were evoked with 100 μM of cineole. Bottom panel: averaged results of 4 – 8 experiments.

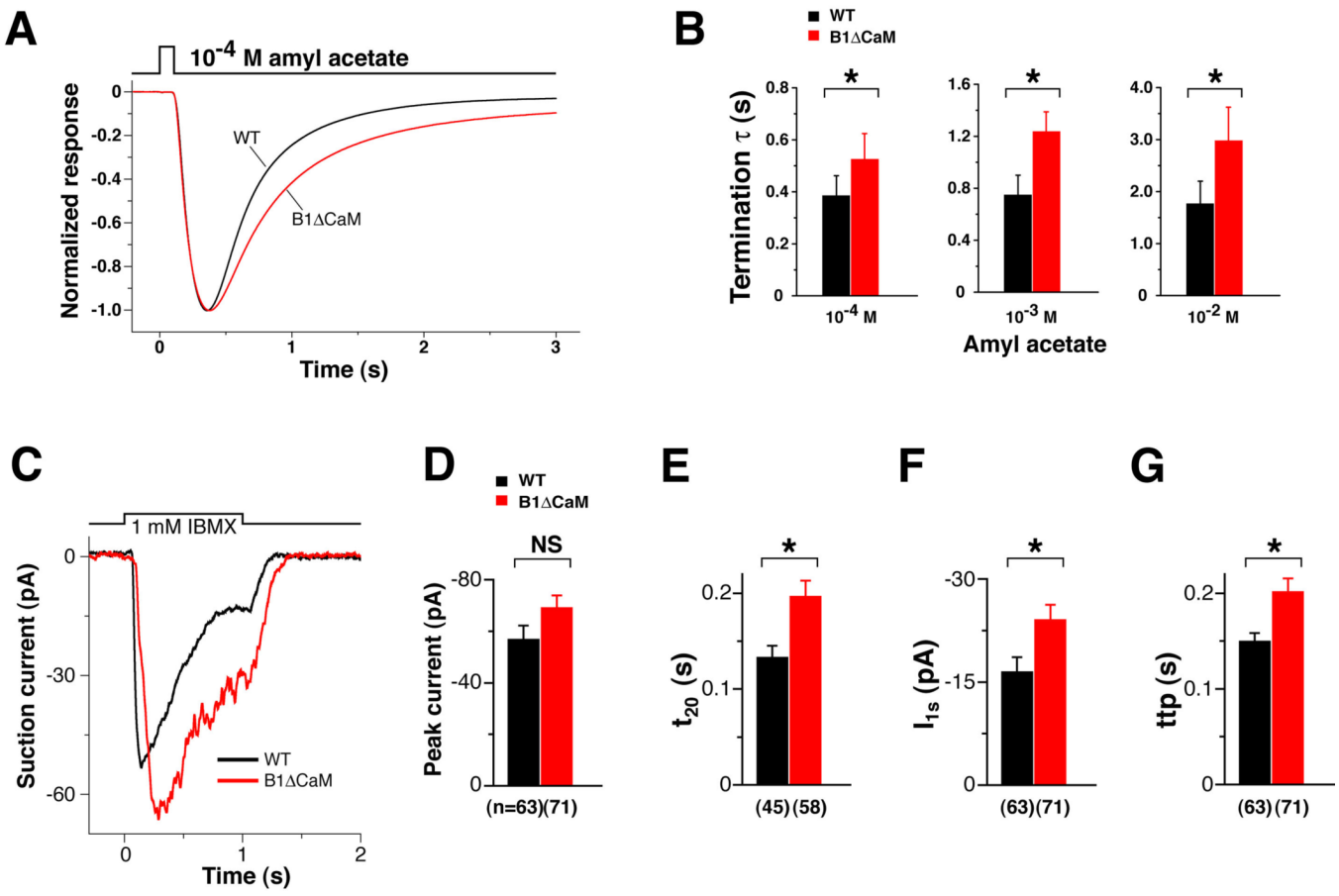

Figure 5. CNGB1$^{\Delta CaM}$ OSNs displayed slower termination kinetics

(A and B) EOG analysis.

(A) Normalized EOG signals to a 100 ms pulse of vapor of 10^{-4} M amyl acetate. The EOG traces of wild type (black) and CNGB1$^{\Delta CaM}$ (red) mice, each the average from 6 animals, are superimposed to show the slower termination phase of CNGB1$^{\Delta CaM}$ mice.

(B) Time constants of the termination phase. The termination phase (100% – 10% peak) of each response was fitted with a single exponential. *, $p<0.05$ for 10^{-4} M; $p<0.01$ for 10^{-3} M and 10^{-2} M (Student's t-test).

(C – G) Single cell suction electrode recordings in response to a 1-second IBMX exposure. Examples of a wild type OSN (black) and a CNGB1$^{\Delta CaM}$ OSN (red) are shown in (C). Collected results from multiple recordings are shown in (D – G).

(D) The difference in the peak current between the two genotypes is not significant (NS, $p=0.05$ Student's t-test). The number of recordings is provided in parenthesis below the graphs.

(E) In CNGB1$^{\Delta CaM}$ OSNs, the time for the current to decline to 20% of the end-perfusion value is significantly longer, meaning slower termination kinetics (*, $p<0.01$).

(F) Consistent with the EOG data (see Figure 8B), CNGB1$^{\Delta CaM}$ OSNs retained significantly larger currents at the end of stimulation compared to wild type, meaning attenuated adaptation (*, $p<0.05$).

(G) Consistent with the EOG data (see Figure 8C), CNGB1$^{\Delta CaM}$ OSNs have a longer time to peak in response to sustained stimulation (*, $p<0.01$).

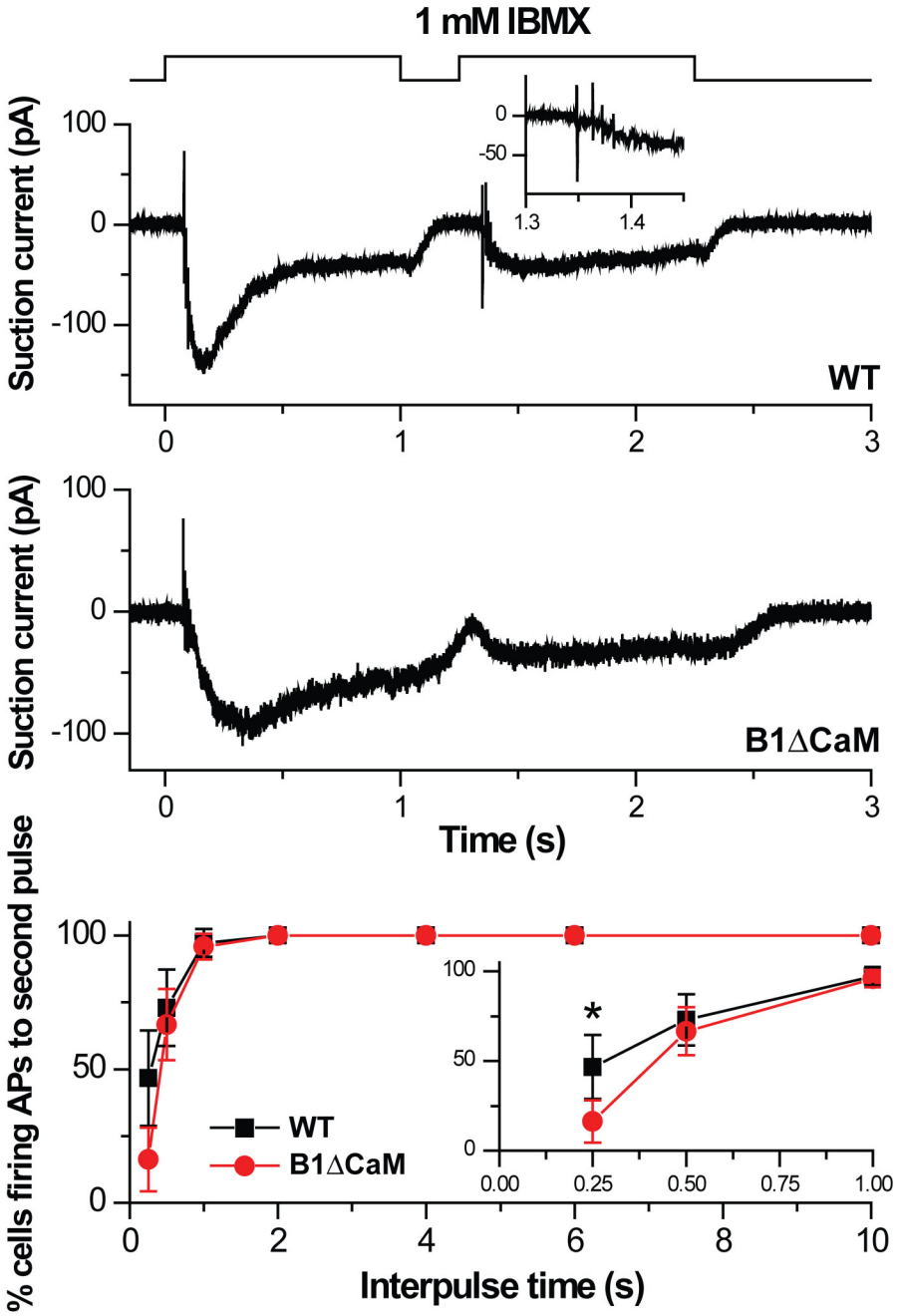

Figure 6. Reduced action potential firing during short recovery periods in CNGB1$^{\Delta CaM}$ OSNs

Suction pipette recordings from an isolated wild type (top panel) or CNGB1$^{\Delta CaM}$ OSN (middle panel) in response to two IBMX pulses (1 mM, 1 second) separated by a 0.25 second interpulse interval. Traces were filtered with the wide bandwidth of DC – 5000 Hz to monitor action potential firing. Inset in the top panel shows the action potential events during the rising phase of the wild type OSN response to the second pulse on an expanded time scale. Note the lack of action potential events in the CNGB1$^{\Delta CaM}$ OSN response to the second pulse. Bottom panel: Percentage of OSNs firing action potentials as a function of the interpulse interval. Inset shows the three shortest interpulse intervals on an expanded time axis. Percentage of cells firing action

potentials is statistically different at the 0.25 second interpulse interval ("*", Chi-square test, p=0.0068). Values are mean ± 95% confidence interval and averages of 19 – 49 OSNs.

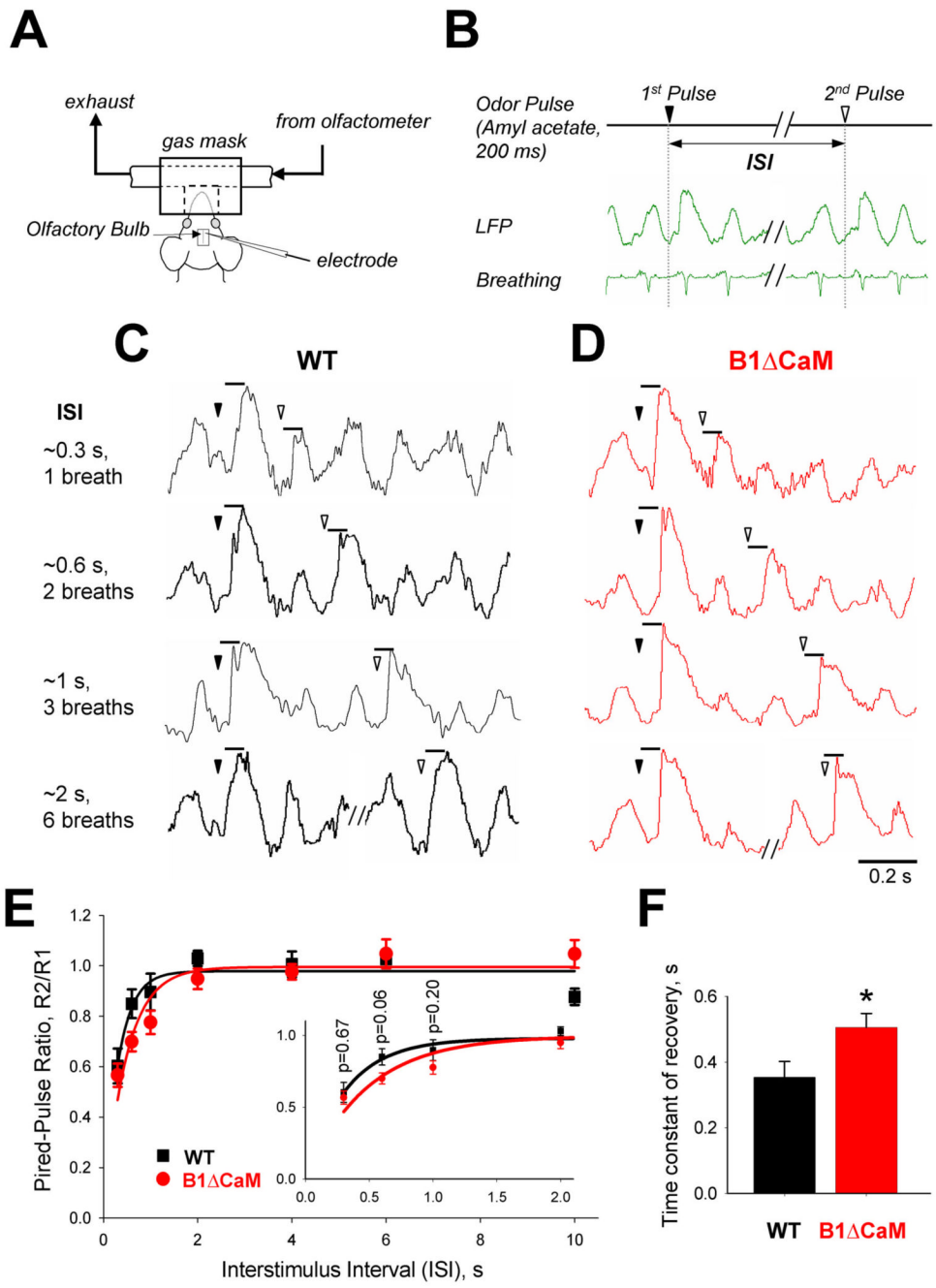

Figure 7. Slower recovery of the odor-evoked local field potentials in the olfactory bulb of CNGB1$^{\Delta CaM}$ mice

(A) Experimental setup for odor stimulation and assessment of field responses in the OB. The recording electrode was positioned in the deep layer of the OB. (B) Two consecutive odor pulses were delivered at the same phase of the breathing cycle. This was achieved in real-time by triggering the olfactometer from piezoelectric sensor attached to the animals' chest. (C and D) Series of representative odor-evoked local field potentials (LFPs) recorded from the OB of the wild type (C) and CNGB1$^{\Delta CaM}$ (D) mice to paired odor pulses separated by 1, 2, 3 and 6 breathing cycles (approximate 0.3, 0.6, 1.0 and 2.0 sec ISI). The triangles denote the start of the first (filled) and the second (open) odor pulses. (E) The average paired-pulse ratios R2/R1

as a function of ISIs for odor-evoked responses (peak amplitude) in the wild type (black squares) and CNGB1$^{\Delta CaM}$ mice (red circles). Each point is an average response from 5 animals in each experimental group ±SE. In each animal, the odor responses are averaged over 5 repetitions. Solid lines represent a single exponential fit to the paired-pulse ratios. Inset shows the four shortest ISI points on an expanded time axis. P values obtained using Student's t-test. (F). Average time constant of LFP recovery (wild type, 0.35±0.042 sec; CNGB1$^{\Delta CaM}$, 0.50 ±0.048 sec). p=0.045, Student's t-test.

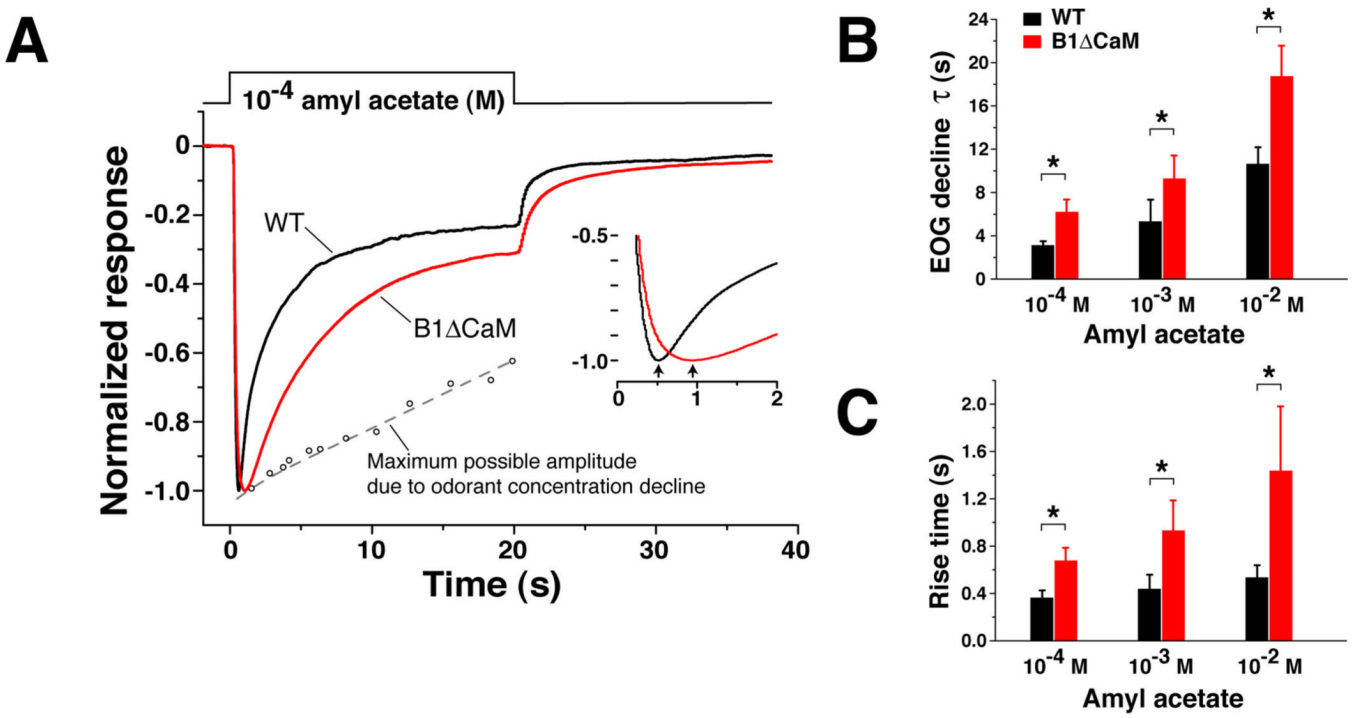

Figure 8. CNGB1$^{\Delta CaM}$ OSNs exhibit reduced adaptation during sustained stimulation

(A) Normalized EOG signals to a 20-second pulse of vapor of 10^{-4} M amyl acetate solution. The EOG traces of the wild type (black) and CNGB1$^{\Delta CaM}$ (red) mice, each the average of recordings from 5 animals, are superimposed to show the attenuated adaptation of the CNGB1$^{\Delta CaM}$ mice during the stimulation. Note that our odorant delivery setup does not deliver a constant odorant concentration as the saturated vapor is diluted during the stimulation period. To assess how the concentration decrease affects the decline of EOG signals, we used a three-way valve to initially divert the odorant stream away from the epithelium and then towards the epithelium at different time points of the 20-second stimulation period. The peak amplitudes obtained are plotted as small open circles fit with an approximating dashed line. The presence of this concentration decrease should affect the tau values in (B). The tau is expected to be larger without this decrease in odorant concentration. Inset, EOG signals plotted from 0 to 2 seconds to show the longer rise time in CNGB1$^{\Delta CaM}$ OSNs. The arrows indicate the peak of the response.

(B) CNGB1$^{\Delta CaM}$ OSNs display slower response decline during sustained stimulation. The decline phase of EOG signals during the stimulation was fit with a single exponential. * $p<0.01$, Student t-test.

(C) CNGB1$^{\Delta CaM}$ OSNs have longer rise times in response to sustained stimulations. *, $p<0.01$.

Table 1

Activation and termination kinetics of EOG responses

Amyl acetate (M)	Latency (ms) to 1% of peak		Rise time (ms) 1%-99% of peak		Termination τ (s) 100%-10%	
	WT	CNGB1$^{\Delta CaM}$	WT	CNGB1$^{\Delta CaM}$	WT	CNGB1$^{\Delta CaM}$
10^{-4}	97±11	98±9	224±17	236±19	0.39±0.08	0.53±0.10 *
10^{-3}	97±11	97±4	281±27	309±17	0.75±0.15	1.24±0.15 *
10^{-2}	92±17	84±5	317±26	366±50	1.77±0.43	3.0±0.64 *

* P<0.05 for 10^{-4} M; P<0.01 for 10^{-3} and 10^{-2} M.